RSC Advances

ROYAL SOCIETY OF CHEMISTRY

www.rsc.org/advances

RSC Advances

RSCPublishing

PAPER

Synthesis and Characterisation of Layered Double Hydroxide Dispersions in Organic Solvents

Cite this: DOI: 10.1039/xoxxoooooox

Miaosen Yang, Olivia McDermott, Jean-Charles Buffet and Dermot O'Hare*

Received ooth January 2012,
Accepted ooth January 2012

DOI: 10.1039/xoxxoooooox

www.rsc.org/

Aqueous Miscible Organic Solvent Treated (AMOST) Mg_3AlCO_3-LDHs have been prepared using twelve different (AMO) solvents. We find that the AMOST process produces significant changes to the crystallinity, morphology, thermal behaviour and dramatically increases the surface areas of the LDHs compared to conventional LDHs. Remarkably AMO-LDHs platelets are now hydrophobic and can be dispersed in a range of organic liquids. Clear dispersions of AMO-Mg_3AlCO_3-LDHs are observed in aromatic solvents. Overall we found the optimum AMO-Mg_3AlCO_3-LDHs organic solvent dispersions are obtained using 1-propanol as a treating solvent and ethyl benzene as the dispersion solvent. This system produces a monophasic dispersion at loading up to 140 g/L of Mg_3AlCO_3-LDH in ethyl benzene. At a maximum loading of 160 g/L Mg_3AlCO_3-LDH this mixture becomes a thick monophasic gel.

Introduction

Conventional layered double hydroxides (LDHs) are a family of compounds containing brucite-like layers with general chemical composition $[M_{1-x}\ M'_x(OH)_2]^{a+}(A^{n-})_{a/n}\bullet bH_2O$, where M is typically a metal divalent and M' is typically a trivalent cation, A^{n-} is an *n*-valent anion.[1] LDHs have captured much attention in recent years due to their impact across a range of applications such as catalysis,[2,3] optics,[4] medical science,[5,6] and in inorganic-organic nanocomposites.[7-10]

However, LDHs synthesised by conventional methods are often highly aggregated due to their high charge density and hydrophobicity. As a result, isolated LDH powders exhibit relatively low surface areas and unmodified forms cannot be dispersed in non-polar liquids, this imposes severe limitations on their ability to disperse in non-polar liquids or polymers and their ability to be surface functionalised.

Recently, we reported a simple novel method, called the Aqueous Miscible Organic Solvent Treatment (AMOST) method, to obtain a new generation of so called "AMO-LDHs. For example, AMO-Mg_3Al-CO_3, AMO-Zn_2Al-Borate and AMO-Mg_3Al-Borate LDHs which are highly dispersible in non-polar hydrocarbon solvents and exhibit high specific surface area (up to 458.6 $m^2.g^{-1}$).[11] In this method, the LDHs are synthesised by conventional methods, eg co-precipitation, but the final wet LDH particle suspension is washed and then dispersed in a 100% aqueous miscible organic (AMO) solvent. In some cases AMO solvent treatment of the LDH can lead to dispersion into thin nanosheets or exfoliation to even single layers.[12-14] Recent studies have shown that AMO-LDHs have a unique chemical composition given by $[M_{1-x}M'_x(OH)_2]^{a+}(A^{n-})_{a/n}\bullet bH_2O\bullet c$(AMO-solvent), which instantly distinguishes them from conventional LDHs.[15] To date, we have focused on the use of acetone and ethanol as the AMO solvents. Here we report a more in depth study of the effect of other AMO solvent treatments on the surface properties of the LDH and their ability to form stable dispersion in range of organic solvents.

Experimental details.

Synthesis of $MgAlCO_3$-LDH using different organic washing solvents. Mg_3AlCO_3-LDH was synthesised using a method adapted from the literature.[11,15a] $Mg(NO_3)_2{\cdot}6H_2O$ (9.60 g, 37.4 mmol) and $Al(NO_3)_3{\cdot}9H_2O$ (4.68 g, 12.5 mmol) were dissolved in 50 mL distilled water (Solution A). A second solution was made using Na_2CO_3 (2.65 g, 25.0 mmol) dissolved in 50 mL distilled water and made to pH 10 by the addition of approximately 5 mL of 1 M HNO_3 (Solution B). Solution A was added to Solution B dropwise over 30 minutes with stirring with the pH maintained at pH 10 using 4 M NaOH. The resulting solution was aged with stirring for 16 hours. After aging, the LDH slurry was washed with distilled water at 70 °C until the pH of the washings was pH 7. The slurry was then washed with 200 mL one of 12 aqueous miscible organic (AMO) solvents {The solvents used were; 1-propanol, 2-propanol, acetone, acetonitrile, dimethylformamide (DMF), dimethylsulfoxide (DMSO), dioxane, ethanol, ethyl acetate (EA), ethylene glycol (EG), methanol and tetrahydrofuran (THF)} and then dispersed in 200 mL of this solvent for one hour. This washing and dispersion process was repeated on the slurry three times. After washing, the slurry was dried for 24 hours in a vacuum oven.

Preparation of dispersions. 0.1 g of LDHs was ground into a fine powder using a pestle and mortar, added to 5 mL of the chosen solvent in a glass vial and sonicated for five minutes. The ultrasonic apparatus (CAT No. H100U) was supplied by Essex Scientific Laboratory Supplies Ltd. The samples were allowed to stand for 10s before the images were taken.

Results and discussion

Characterisation of AMO-Mg_3AlCO_3-LDHs

Mg_3AlCO_3-LDH was synthesised by co-precipitation method. Prior to drying, samples were treated with twelve different AMO solvents. . For comparison, a conventional water-washed Mg_3AlCO_3--LDH sample was also prepared. The powder X-ray diffraction patterns for the thirteen different samples are displayed in Fig. 1 and S1-8.

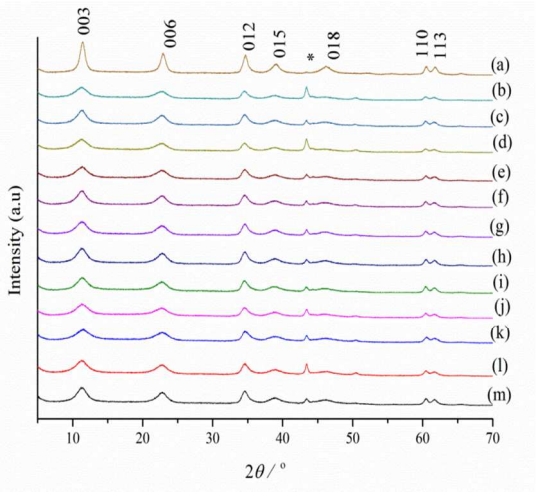

Fig. 1 Powder X-ray diffraction patterns of $MgAlCO_3$-LDH with (a) Water, (b) 1-propanol, (c) 2-propanol, (d) Acetone, (e) Acetonitrile, (f) DMF, (g) DMSO, (h) Dioxane, (i) Ethanol, (j) EA, (k) EG, (l) Methanol and (m) THF as washing solvent. *is an Bragg reflection from the Al sample holder.

Fig. 1 demonstrates that basic LDH structure is unchanged when the washing solvent is changed from water to an aqueous-miscible solvent. The d-spacing of the 003 Bragg reflection remains *ca*. 7.9 Å and d-spacing of the 110 Bragg reflection is unchanged from the expected value of 1.5 Å.[16] These data indicate that there is no detectible intercalation or swelling of the LDH on AMO-solvent treatment. However, the Bragg reflection peak widths indicate that the crystallinity of the Mg_3AlCO_3-LDH is affected when the washing solvent is changed from water to a aqueous-miscible solvent.[17] The Scherrer equation can be used to provide an estimate of the mean crystallite domain length (CDL).[18a] An alternative analysis of particle size can be carried out using a whole-pattern fitting method developed by Pielaszek.[19] The results of both these analyses are collated in Table 1.

Table 1. Mean crystallite domain lengths and sizes for the different solvent washed LDHs.

Washing Solvent	CDL (Å)[a]	CDL (Å)[b]	Mean size (Å)[c]
Water	217.0	629.4	125
1-propanol	145.7	654.8	80
2-propanol	104.4	663.2	78
Acetone	127.3	636.4	68
Acetonitrile	121.2	651.9	71
Dioxane	138.5	669.8	71
DMF	147.0	630.0	77
DMSO	126.6	652.7	77
Ethanol	135.8	631.1	74
EA	136.2	645.3	71
EG	130.6	639.9	69
Methanol	137.4	658.2	76
THF	122.5	638.7	77

[a]along *c*-axis, using the *003* Bragg reflection. [b]in *ab*-plane, using the *110* Bragg reflection. [c]Pielaszek method.[31]

These two different methods give different absolute values for the crystallite size; however the crystallinity along the *c*-axis and the mean particle size show the same overall trend which suggests a reduction in the stacking length of the LDH nanoplates.[18a] The crystallinity in the *ab*-plane is largely unchanged with the variation of washing solvent.

Fig. 2 shows the TEM images for a water-washed and an ethanol-washed LDHs.

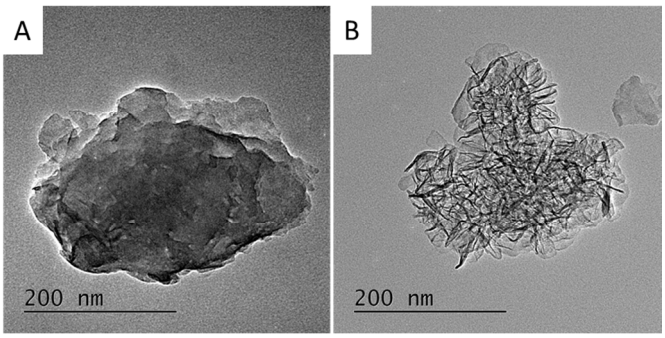

Fig. 2 TEM image of (A) water-washed and (B) ethanol-washed $MgAlCO_3$-LDH.

The darker areas on the TEM image indicate the stacking of the LDH nanosheet crystallites perpendicular to the sample stage. The reduction in these darker areas when the solvent is changed from water to a water-miscible solvent suggests that there is less stacking of the LDH nanosheets, which is consistent with the proposed AMOST mechanism.[11]

The FTIR spectrum for the ethanol-washed Mg_3AlCO_3-LDH is displayed in Fig. S9, it is representative of the IR spectra for all the AMO-LDH synthesised (S10-17). The broad absorption at around 3400 cm^{-1} is caused by the vibrations and stretching modes associated with –O-H bonds. The absorption at around 1630 cm^{-1} corresponds to the bending mode of water, indicating that there is still some water present in the samples, even after treatment with an aqueous-miscible solvent. The absorption at around 1360 cm^{-1} is due to the asymmetric stretching mode of the intercalated carbonate. The absorptions below 1000 cm^{-1} are due to M-O vibrational modes.[20]

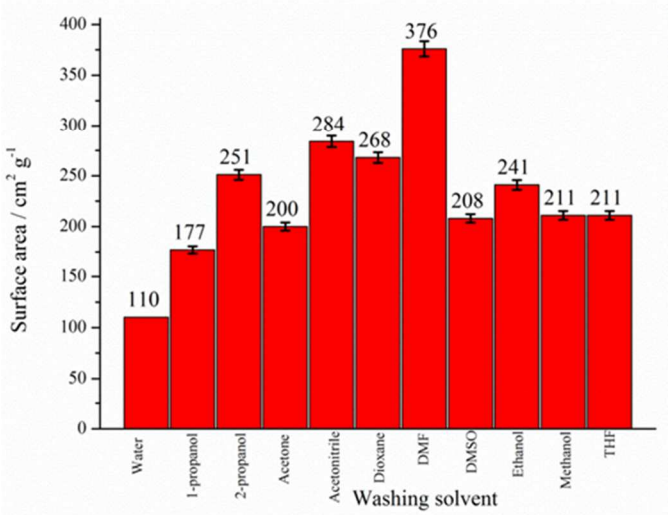

Fig. 3 Nitrogen BET surface areas for the different solvent-treated AMO-Mg_3AlCO_3-LDHs. 2 % error bars are given. The value for the conventional water-washed LDH is from the literature.[11]

Surface area analysis of the AMO-Mg_3AlCO_3-LDHs was performed using using N_2 BET. The measured surface areas for the LDHs washed with different AMO-solvents is summarised in Fig. 3 It is clear that a change in the washing solvent leads to a dramatic variation in the surface area of the LDH product, all the AMO-LDHs are significantly increased surface area compare to the conventional water-washed sample. The DMF washed Mg_3AlCO_3-LDH shows the largest surface area of 376 cm^2/g, which is 3.4 times greater that a conventional water washed sample.

Thermogravimetric analysis (TGA) was used to analyse the thermal decomposition of LDHs. The TGA plots for all samples are displayed in Fig. 4.

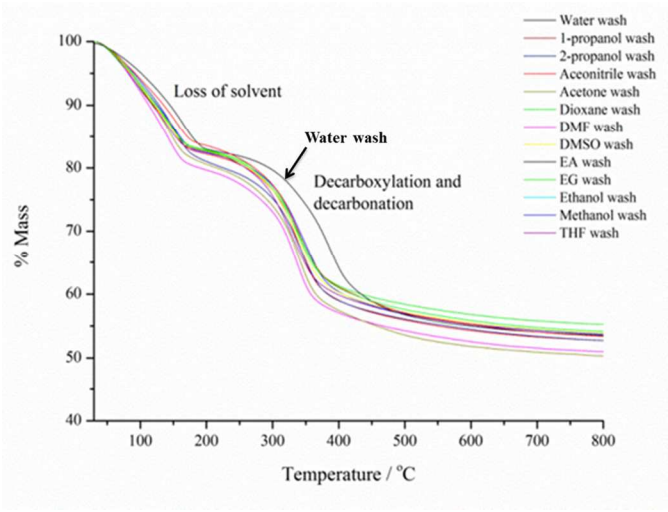

Fig. 4 TGA data for the AMO-$MgAlCO_3$-LDHs.

The mass loss curves for the AMO Mg_3AlCO_3-LDHs all share the same characteristic profile expected for the decomposition of an LDH. However, there are some significant differences between the thermal behaviour of water-washed and AMO-solvent washed LDHs in terms of temperature of mass loss and the gradient of the curve. Taking the first derivative of the TGA curves (dTGA) allows changes in mass to be seen more easily, Fig. 5.

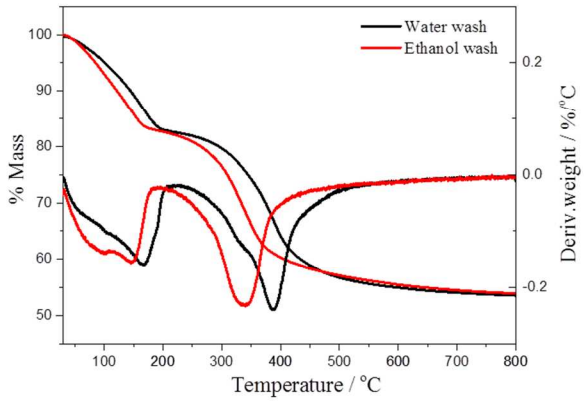

Fig. 5 TGA and dTGA curves for water-washed and ethanol-washed $MgAlCO_3$-LDH.

The dTGA curve of the water-washed sample is typical of unmodified hydrotalcite.[21] The mass loss at *ca.* 165 °C corresponds to the loss of strongly bound interlayer water. The event at 386 °C corresponds to the almost simultaneous dehydroxylation and decarbonation of the LDH; it is believed that the two peaks overlap. The dTGA curve for the ethanol-washed sample shows two well defined events at low temperature, indicating the presence of weakly bound solvent. The mass loss of interlayer water takes place at 145 °C and decarboxylation and dehydroxylation take place at around 340 °C. These are both at a lower temperature than the water-washed sample, which indicates that the interlayer solvent and any remaining water molecules are less strongly bound.[22]

Consistent with the TEM and BET results, the thinner nanosheets and higher surface area of AMO-LDHs also leads to a lower decomposition temperature. Furthermore, we find an additional reproducible feature in the TGA of AMO-LDHs. Different from water-washed sample, there is another small endothermic step between 90-110 °C, which is caused by the ethanol adsorbed on the LDH surface. We find this feature in all AMO-LDHs (see Fig. S18-26). This signature enable us do have define a new compositional formula for this family: $[M_{1-x}M'_x(OH)_2]^{a+}(A^{n-})_{a/n}\bullet bH_2O\bullet c$(AMO-solvent). The details of the composition determined for each AMO-LDH and water-washed LDH are listed in Table S2.

Organic solvent dispersions of AMO-Mg_3AlCO_3-LDHs

We have previously reported that acetone treated Mg_3AlCO_3-LDH may be dispersed in xylenes. We were interested to determine if the different AMO solvent treatment of Mg_3AlCO_3-LDH would affect their ability to disperse in other liquid solvents. The twelve different AMO solvent treated AMO-Mg_3AlCO_3-LDHs were then dispersed in eleven different solvents. The aromatic solvents chosen were *o*-xylene, *p*-xylene, toluene, tetrahydrofuran (THF), dimethylformamide (DMF) and ethyl benzene in addition to several other non-aromatic solvents 1-methyl-2-pyrrolidone, dichloromethane (DCM), dimethylsulfoxide (DMSO), chloroform and ethanol.

In each case a 20 g/L loading of the AMO-Mg_3AlCO_3-LDHs were prepared. The dispersions fell into two classes: opaque and transparent. An example of each is depicted in Fig. 6 which shows a 20 g/L acetone-washed Mg_3AlCO_3-LDHs dispersed in *o*-xylene, Fig. 6 (A) and the equivalent amount dispersed in ethanol, Fig. 6 (B).

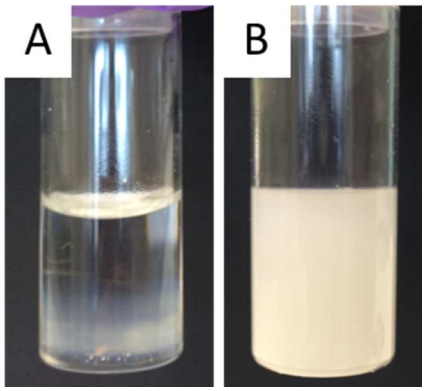

Fig. 6 20 g/L of acetone-washed Mg_3AlCO_3-LDH dispersed in (A) *o*-xylene and (B) ethanol.

The only dispersions which were optically transparent were AMO-$MgAlCO_3$-LDHs dispersed in the aromatic solvents; ethyl benzene, *o*-xylene, *p*-xylene and toluene, each of these dispersions exhibited the Tyndall effect.[23] On standing at room temperature these dispersions were observed to settle into two distinct layers, with the upper layer showing a very weak Tyndall effect and the lower layer showing a high degree of light scattering.

Table 2. Observations on selected LDH dispersions

Washing Solvent	Dispersion Solvent	Time for separation	Lower layer description
1-propanol	Ethyl benzene	6 hours	Very clear, only slightly less transparent than upper layer
2-propanol	Toluene	20 seconds	White, solid-like, making up more than half the sample
Acetone	*o*-xylene	2 hours	Translucent, pearlescent

Acetonitrile	*p*-xylene	24 hours	Translucent, pearlescent
Ethylene glycol	*o*-xylene	1 minute	Thick layer of white solid
Methanol	*p*-xylene	24 hours	Translucent, almost opaque

The time taken for the dispersions to settle varied between each AMO-treated LDH from a few seconds to 24 hours. The behaviour of selected dispersions are summarised in Table 2. Four full observations are recorded in Table S1. For some samples, the lower layer was translucent and pearlescent in appearance whereas for others the lower layer was opaque. An example of each is shown in Fig. 7. Neither type of dispersion is stable at this loading and so do not stay as single transparent phase.

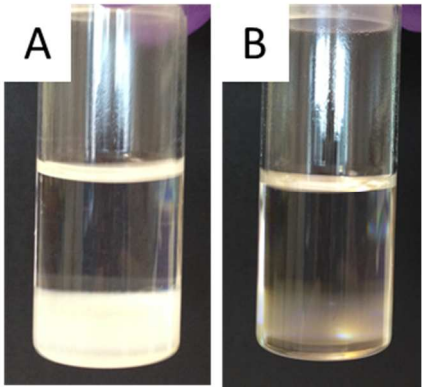

Fig. 7: (A) Images of acetonitrile-washed $MgAlCO_3$-LDH dispersed at 20 g/L in toluene, (B) THF-washed $MgAlCO_3$-LDH dispersed at 20 g/L in toluene.

The results indicate that there is complex phase behaviour for these LDH dispersions. One would expect the dispersions to follow the normal phase behaviour for a regular solution, where at a single temperature the system may be mono- or biphasic (with a solid and a liquid phase) depending on the mole fraction of the solvent. For some two phase systems, there is a point where both phases are truly liquid rather than being a solid phase and a liquid phase. Dispersions similar to Fig. 7 (a) appear to be made up of an upper liquid layer and a lower colloidal layer.

A single dispersion with a transparent lower phase was selected and monitored over the course of one week. Fig. 8 shows acetone-washed $MgAlCO_3$-LDH dispersed in *o*-xylene after initial dispersion and after one week. Additional photographs are provided in Fig. SI27.

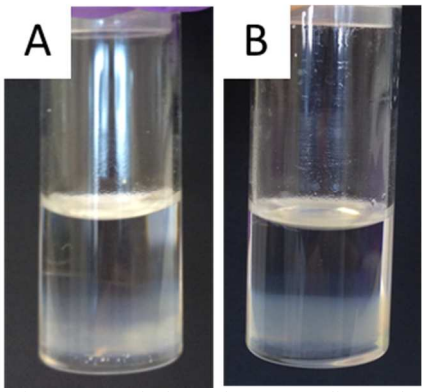

Fig. 8 Images of acetone-washed $MgAlCO_3$-LDH dispersed at 20 g/L in *o*-xylene, (A) initial dispersion and (B) after 1 week.

After settling from the initial single translucent phase into a clear, predominately solvent phase and a lower colloidal phase, the separation remains stable, with no visible LDH crystallites. This may indicate that a true liquid-liquid phase separation has been achieved. Different AMO washing and dispersing solvent combinations lead to different phase behaviour for these dispersions, indicating that there are interactions between the two different solvents and the solid LDH which influence the clarity and stability of the dispersion.

The dispersions which appeared clear after initial addition of LDH display the Tyndall effect were then investigated using UV-vis spectroscopy. The clarity or turbidity was determined by measuring percentage transmittance (T%) between 800 and 200 nm. To aid comparison, T% of the dispersions at 500 nm was recorded.[8] Three measurements were taken; the dispersion immediately after agitation, and the upper and lower layers once the dispersion had settled. Results for dispersions in ethyl benzene and *o*-xylene are summarised in Fig. 9 and 10. Results for dispersions in *p*-xylene and toluene are displayed in Fig. S28 and S29 respectively.

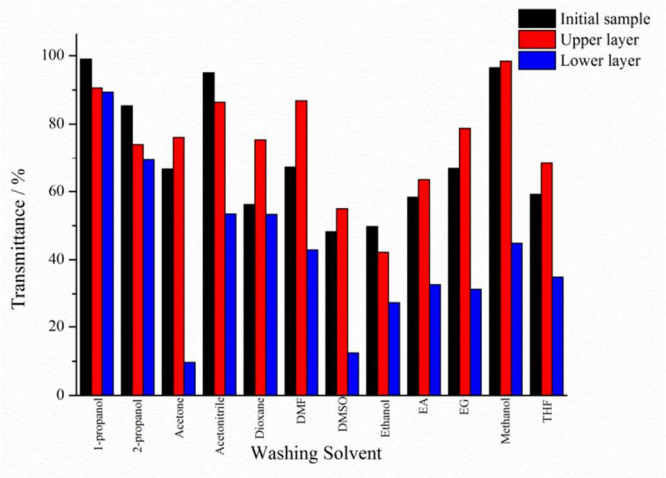

Fig. 9 Transmission factor (%) at 500 nm of ethyl benzene dispersions at 20 g/L for AMO-Mg_3AlCO_3 LDH treated with a range of organic solvents.

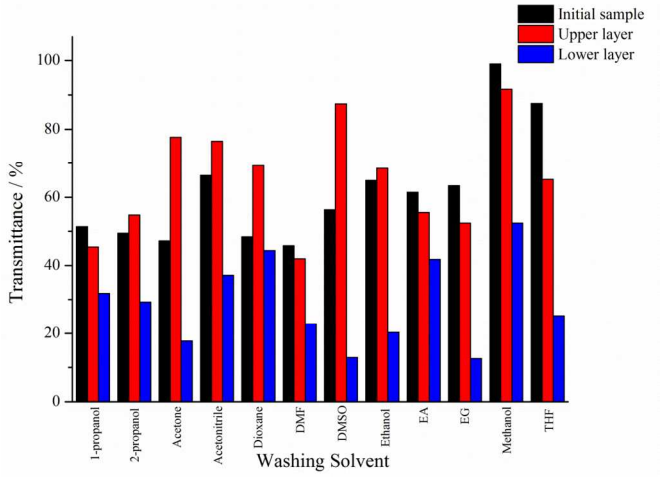

Fig. 10 Transmission factor (%) at 500 nm for *o*-xylene dispersions at 20 g/L for AMO-Mg_3AlCO_3 LDH treated with a range of organic solvents.

A 'good' dispersion was defined as one with high transparency (T% $\geq$ 50%) in both the initial dispersion and the lower layer of the biphasic system. We can use optical clarity is a measure of how well dispersed LDHs are in each solvent. If the lower phase is not colloidal, it will show very low transparency; the 'best' dispersions will be those where the lower layer is most transparent, as this will indicate a high level of dispersion of the LDH. The lower layer was also examined visually to check if any large aggregates of LDH

particles formed. For example, 2-propanol-washed LDH produces a good dispersion on addition to ethyl benzene (T% = 85.4% in initial sample and 74.1% in lower layer) and DMSO-washed LDH forms a poor dispersion in *o*-xylene (T% = 56.3% in initial dispersion and 12.9% in lower layer). For each dispersion solvent, an optimum pairing was selected for further investigation. The pairings were: 1-propanol-washed LDH in ethyl benzene, methanol-washed LDH in *o*-xylene, methanol-washed LDH in *p*-xylene and acetonitrile-washed LDH in toluene.

With each of the optimum pairings, an investigation was carried out into the effect of increasing the LDH loading on the biphasic character, transparency and thickness of the dispersions. Fig. 11 and 12 show how T% changed with increasing loading for 1-propanol-washed LDH dispersed in ethyl benzene and acetonitrile-washed LDH dispersed in toluene. Data for dispersions of methanol-washed LDH in *o*- and *p*-xylene are displayed in Fig. S30 and S31 respectively.

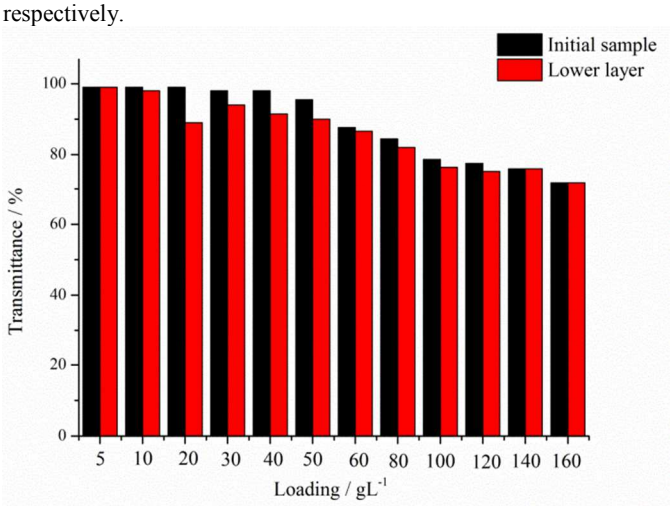

Fig. 11 The variation in transmission factor (%) at 500 nm of increasing loading for 1-propanol-washed Mg_3AlCO_3 dispersed in ethyl benzene.

For 1-propanol-washed LDH dispersed in ethyl benzene, Fig. 11, the biphasic character was optically difficult to identify up to a loading of 40 g/L, but was detected using UV-vis spectroscopy from 10 g/L loading (T% upper layer = 99.4%, T% lower layer = 98.0%). At a loading of 140 g/L, the dispersion became monophasic (ΔT% = 0). Maximum loading was achieved at 160 g/L, when the sample became a thick, monophasic gel.

For acetonitrile-washed LDH dispersed in toluene, Fig. 12, the dispersion did not display biphasic character until 20 g/L loading (T% upper layer = 96.5%, T% lower layer = 76.8%). At a loading of 50 g/L, it became a single translucent phase and a thick, translucent gel (ΔT% = 0). For methanol-washed LDH in *o*-xylene, biphasic character was not apparent until 10 g/L loading, Fig. SI5. At a loading of 70 g/L it became a single translucent phase, and at 90 g/L it became a thick translucent gel. For methanol-washed LDH in *p*-xylene, biphasic character was observed for all loadings up to 60 g/L, when a single translucent phase was seen, Fig. SI6. The dispersion thickened with loading and became an immobile gel at a loading of 80 g/L.

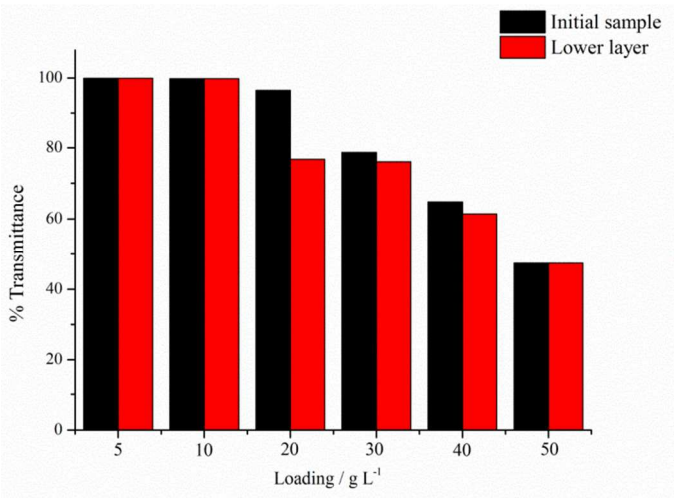

Fig. 12 The variation in transmission factor (%) at 500 nm of increasing loading for acetonitrile-washed Mg_3AlCO_3 LDH dispersed in toluene.

'Good' dispersions were those that showed high transparency in the initial sample and of the lower phase once the sample had settled into two phases. Reasons for favourable dispersion properties are likely to be related to the properties of the solvent used for washing or the interaction between the washing and dispersion solvent. There does not appear to be a correlation between the polarity of the washing solvent and the dispersion solvent for dispersions that showed a high level of transparency. For the 'best' pairings that were investigated, the boiling point of the washing solvent was lower than the boiling point of the dispersion solvent. LDHs washed with solvents with boiling points higher than the dispersion solvent dispersed poorly (e.g. DMF and DMSO).

Properties of the LDH obtained after washing (*e.g.* a change in surface area) may also be a factor in how well the LDH disperses. However, the LDHs which gave the most transparent dispersions display very different surface areas; 1-propanol-washed $MgAlCO_3$-LDH had the smallest surface area at 177 cm^{-1}, whilst acetonitrile-washed $MgAlCO_3$-LDH exhibited a very large surface area of 284 cm^{-1}.

Conclusions

Aqueous Miscible Organic Solvent Treated (AMOST) Mg_3AlCO_3-LDHs have been prepared using twelve different organic treatment solvents. The AMOST process produces significant changes to the crystallinity, morphology, thermal behaviour and dramatic increases the surface areas of the LDHs.

AMOST-modified $MgAlCO_3$-LDH can form clear dispersions in a range of aromatic solvents at high loadings. To date, our experiments concluded that the optimal dispersion is a 1-propanol treated Mg_3AlCO_3-LDHs dispersed in ethyl benzene. This system produces a monophasic dispersion at loading up to 140 g/L in ethyl benzene. At a maximum loading of 160 g/L, this mixture becomes is a thick monophasic gel.

Acknowledgements

M.Y. and J.-C.B. would like to thank SCG Chemicals Ltd, Thailand for funding.

Notes and references

Chemistry Research laboratory, 12 Mansfield Road, OX1 3TA Oxford, UK. E-mail: Dermot.ohare@chem.ox.ac.uk

Electronic Supplementary Information (ESI) available: [experimental details, characterisations]. See DOI: 10.1039/b000000x/

1 (a) X. Duan and D. G. Evans, *Layered double hydroxides*, *Springer Verlag*, 2006; (b) V. Rives, *Layered double hydroxides: present and future*, Nova Science Publishers, 2001; (c) F. Cavani, F. Trifiro and A. Vaccari, Catal. Today, 1991, **11**, 173.
2 X. Zou, A. Goswami and T. Asefa, *J. Am. Chem. Soc.*, 2013, **135**, 17242.
3 Y. Zhao, B. Li, Q. Wang, W. Gao, C. J. Wang, L. Zheng, M. Wei, D. G. Evans, D. G., X. Duan and D. O'Hare, *Chem. Sci.*, 2014, **5**, 951.
4 Z. Liu, R. Ma, M. Osada, N. Iyi, Y. Ebina, K. Takada and T. Sasaki, *J. Am. Chem. Soc.*, 2006, **128**, 4872.
5 X. Gao, L. Lei, D. O'Hare, J. Xie, P. Gao and T. Chang, *J. Solid State Chem.*, 2013, **203**, 174.
6 J.-H. Choy, S.-Y. Kwak, Y.-J. Jeong and J.-S. Park, *Angew. Chem. Int. Ed.*, 2000, **39**, 4042.
7 (a) Q. Wang, J. Undrell, Y. Gao, G. Cai, J.-C. Buffet, C. A. Wilkie and D. O'Hare, *Macromolecules*, 2013, **46**, 6145. (b) Y. Gao, J. Wu, Q. Wang, C. A. Wilkie and D. O'Hare, *J. Mater. Chem. A*., 2014, **2**, 10996.
8 Q. Wang, X. Zhang, J. Zhu, Z. Guo and D. O'Hare, *Chem. Commun.*, 2012, **48**, 7450.
9 S. Abedi and M. Abdouss, *Appl. Cat. A*., 2014, **475**, 386.
10 (a) Y. Gao, Z. Zhang, J. Wu, X. Yi, A. Zheng, A. Umar, D. O'Hare and Q. Wang, *RSC Adv*., 2013, **3**, 26017. (b) F.-A. He and L.-M. Zhang, *Compos. Sci. Technol.*, 2007, **67**, 3226. (c) F.-A. He and L.-M. Zhang, *J. Colloid Interface Sci.*, 2007, **315**, 439.
11 Q. Wang and D. O'Hare, *Chem. Commun., 2013,* **49**, 6301.
12 K. Li, G. Wang, D. Li, Y. Lin and X. Duan, *Chinese J. Chem. Eng.*, 2013, **21**, 453.
13 (a) J. Oh, S. Hwang and J. Choy, *Solid State Ionics*, 2002, **151**, 285. (b) A. Alvarez, R. Trujillano and V. Rives, *Appl. Clay. Sci*., 2013, **80-81**, 326.
14 (a) S. Zeng, X. Xu, S. Wang, Q. Gong, R. Liu and Y. Yu, *Mater. Chem. Phys.*, 2013, **140**, 159. (b) Z. Huang, P. Wu, B. Gong, Y. Fang and N. Zhu, *J. Mater, Chem. A*, 2014, **2**, 5534. (c) L. chen, K. Sun, P. Li, X. Fan, J. Sun and S. Ai, *Nanoscale*, 2013, **5**, 10982. (d) H. Chen, L. Hu, M. Chen, Y. Yan and L. Wu, *Adv. Func. Mater*., 2014, **24**, 934. (d) Z. Hu and G. Chen, *RSC Advances*, 2013, **3**, 12021. (e) Z. P. Xu, G. Stevenson, C.-Q. Lu and G. Q. M. Lu, *J. Phys. Chem. B*, 2006, **110**, 16923.
15 (a) C. Chen, M. Yang, Q. Wang, J.-C. Buffet and D. O'Hare, *J. Mater. Chem. A*., 2014, DOI: 10.1039/c4ta02277g. (b) N. P. Funnell, Q. Wang, L. Connor, M. G. Tucker, D. O'Hare and A. L. Goodwin, *Nanoscale*, 2014, **6** , 8032. (c) Q. Wang and D. O'Hare, *Chem. Rev.*, 2012, **112**, 4124.
16 (a) Q. Tao, H. He, R. L. Frost, P. Yuan and J. Zhu, *J. Therm. Anal. Calorim.*, 2009, **101**, 153. (b) B. Kutlu, A. Leuteritz, R. Boldt, D. Jehnichen and G. Heinrich, *Chem. Eng. J.*, 2014, **243**, 394.
17 G. Hu, N. Wang, D. O'Hare and J. Davis, *J. Mater. Chem.*, 2007, **17**, 2257.
18 R. E. Dinneier and S. J. L. Billinge, S. J. L. Principles of Powder Diffraction. In *Powder Diffraction: Theory and Practice*; R. E. Dinneier and S. J. L. Billinge; Eds.; Royal Society of Chemistry, 2008; pp. 1-19 (b) J. I. Langford and A. J. C. Wilson, *J. Appl. Crystallogr.,* 1978, **11**, 102. (c) Q. Wang, X. Zhang, C. J. Wang, J. Zhu, Z. Guo and D. O'Hare, *J. Mater. Chem.*, 2012, **22**, 19113.
19 (a) R. Pielaszek, *J. Alloys Compd.*, 2004, **382**, 128. (b) T. Wejrzanowski, R. Pielaszek, A. Opalińska, H. Matysiak, W. Łojkowski and K. J. Kurzydłowski, *Appl. Surf. Sci.*, 2006, **253**, 204.
20 (a) Q. Tao, J. Zhu, R. L. Frost, T. E. Bostrom, R. M. Wellard, J. Wei, P. Yuan and H. He, *Langmuir*, 2010, **26**, 2769. (b) Q. Tao, J. Zhu, R. M. Wellard, T. E. Bostrom, R. L. Frost, P. Yuan and H. He, *J. Mater. Chem.*, 2011, **21**, 10711. (c) A. de Roy, C. Forano and J. P. Besse, Layered Double Hydroxides: Synthesis and Post-Synthesis Modification. In *Layered Double Hydroxides: Present and Future*; V. Rives, Ed.; Nova Publishers, 2001; pp. 39-50.
21 F. L. Theiss, G. A. Ayoko and R. L. Frost, *J. Therm. Anal. Calorim.*, 2012, **112**, 649.
22 (a) S. Palmer, R. Frost and T. Nguyen, *Coord. Chem. Rev.*, 2009, **253**, 250. (b) F. Malherbe, J.-P. Besse, *J. Solid State Chem.*, 2000, **155**, 332.
23 D. Ebbing and S. D. Gammon, *General Chemistry, Enhanced Edition*; Cengage Learning, 2010; p. 509.

